Research Square

Preprints are preliminary reports that have not undergone peer review.
They should not be considered conclusive, used to inform clinical practice,
or referenced by the media as validated information.

Carboxymethyl cellulose aerogels with Laponite, halloysite or kaolin: effect of clay type on shrinkage, compressive and heat-transfer behavior

Onur Aras
Istanbul Medeniyet University
Samed Ozaydin
Istanbul Medeniyet University
Enes Atas
Istanbul Medeniyet University
Murat Kazanci
muratkazanci.tr@gmail.com

Istanbul Medeniyet University

Research Article

Keywords: Cellulose ether, Polysaccharide nanocomposite, Smectite, Kaolinite, Ice templating, Thermal barrier

Posted Date: November 6th, 2026

DOI: https://doi.org/10.21203/rs.3.rs-10481000/v1

License: This work is licensed under a Creative Commons Attribution 4.0 International License.
Read Full License

Additional Declarations: No competing interests reported.

Abstract

Freeze-dried carboxymethyl cellulose aerogels are light but can shrink during drying and are mechanically weak. This study examined how the type of clay changes the structure and properties of these aerogels, comparing the synthetic smectite Laponite (2:1 layered discs) with the 1:1 aluminosilicates halloysite (nanotubes) and kaolin (platelets). A 0.8% (w/v) carboxymethyl cellulose solution was mixed in equal volumes with clay dispersions of 0.4–2.0% (w/v) and freeze-dried. Compressive behavior was assessed by uniaxial compression, heat transfer by infrared thermography on a 200°C hot plate, and polymer–clay interactions by Fourier-transform infrared spectroscopy. Aerogels containing Laponite retained about 37% of their cast volume, compared with about 20% for those containing halloysite or kaolin. Because the compression tests ended at very different strains, the composites were compared at 10% strain. At this strain, the Laponite composites carried 2.6–10.3 kPa, 2.0–7.7 times more than the halloysite and kaolin composites, and the stress increased with Laponite concentration, whereas the halloysite and kaolin composites, which have nearly the same composition but different shapes, behaved similarly (1.2–1.6 kPa). After 30 min on the hot plate, the lowest top-surface temperatures (81.6–82.9°C, compared with 90.1°C for the neat aerogel) were recorded for 2.0% halloysite and 1.2–1.6% kaolin. The results suggest that Laponite forms a continuous network with the polymer that limits shrinkage and stiffens the aerogel, whereas halloysite and kaolin act mainly as fillers. As thermal conductivity and porosity were not measured and heights and densities were estimated, the results describe comparative trends.

Introduction

The increasing severity of environmental problems and the urgent need for sustainable materials have directed scientific research toward developing eco-friendly alternatives. The widespread use of petroleum-based plastics causes significant harm to nature and living organisms, driving a global demand for biodegradable materials. Biodegradable materials, particularly those derived from renewable natural resources like cellulose, play a crucial role in reducing environmental impact because they can naturally decompose through microbial action without leaving toxic residues.

Despite their vital environmental benefits, the application areas of biodegradable materials are often restricted due to their inherent limitations in mechanical strength and thermal stability. To overcome these structural shortcomings, researchers have increasingly turned to nanotechnology-based solutions, specifically the development of nanocomposites (Darder et al. 2007). By reinforcing biopolymer matrices with nanofillers, the mechanical durability, thermal resistance, and barrier properties of the materials can be significantly improved, making them viable competitors to traditional plastics (de Oliveira and Beatrice 2018).

Carboxymethyl cellulose (CMC) is a semi-synthetic, water-soluble and biodegradable polymer obtained by chemical modification of cellulose (Günal 1999; Stenstad et al. 2008). Because of its film-forming and stabilizing properties, CMC is a suitable matrix for aerogels, which are highly porous, lightweight

materials with potential for insulation and biomedical applications (Wan et al. 2015; Rahmanian et al. 2021). Cellulose-based aerogels and foams can be good thermal insulators (Wicklein et al. 2015; Fleury et al. 2020), but neat polysaccharide aerogels are often mechanically fragile (Gawryla et al. 2009) and, because of their low solids content, can shrink considerably during freezing and drying. One way to improve them is to combine CMC with inorganic clay minerals to form bionanocomposites (Almasi et al. 2010; Bozoğlan et al. 2020, 2021). Our group has previously modified CMC and other cellulosic matrices by other routes, for example CMC/poly(vinyl alcohol) fibrillar membranes produced by centrifugal spinning (Ataş et al. 2025) and self-reinforced composites of hemp cellulose and cellulose nanocrystals (Aras et al. 2025).

The performance of such composites depends on the type of clay, which determines its layer structure, chemical composition, surface charge and particle shape. Laponite, a synthetic hectorite, is a 2:1 layered magnesium silicate of the smectite group that swells in water into nanometer-sized discs with a high specific surface area and surface charge and can form a physical network within polymer matrices (Can 2008; Jin et al. 2018; Tomás et al. 2018; López-Angulo et al. 2020). Halloysite and kaolinite are both 1:1 aluminosilicates with essentially the same composition, $Al_2Si_2O_5(OH)_4$, but they differ in shape. Halloysite is a hydrated form with a nanotubular structure that has been widely used as a filler and carrier in polymer systems (Joussein et al. 2005; Lvov et al. 2008; Keskin 2016; Yang et al. 2017). Kaolin, composed mainly of the plate-like mineral kaolinite, is a low-cost filler that can improve the thermal stability and compactness of polymer matrices (Prasad et al. 1991; Aroke et al. 2013; Özhan 2017; Nieto et al. 2022).

In CMC, the carboxylate groups along the chain give the polymer a negative charge, and how these groups interact with a clay depends on the surface charge of the clay: Laponite discs carry negative faces and positive edges, whereas the outer surfaces of halloysite tubes and kaolinite platelets are mainly negatively charged (Lvov et al. 2008; Tomás et al. 2018). A clay may therefore either become part of the CMC network or remain a passive filler within it. Because halloysite and kaolin have nearly the same composition but different particle shapes, whereas Laponite differs in composition, surface charge and particle size, comparing the three clays in the same CMC aerogel system, prepared under identical conditions, can show whether particle shape or clay chemistry governs how the CMC network responds. The aim of this study was therefore to prepare CMC aerogels containing 0.4–2.0% (w/v) Laponite, halloysite or kaolin, to determine how the clay type changes the shrinkage of the CMC network during freeze-drying, its compressive behavior and its heat transfer under a fixed thermal load, and to examine the polymer–clay interactions by FTIR spectroscopy.

Materials and methods

Materials

Sodium carboxymethyl cellulose (Sigma-Aldrich, St. Louis, MO, USA), Laponite RD (BYK-Chemie GmbH, Wesel, Germany), halloysite (Eti Maden, Türkiye) and kaolin (AlfAsol, Türkiye) were used as received

without further purification. Deionized water was used throughout.

Preparation of CMC aerogels and selection of the CMC concentration

Aqueous CMC solutions were prepared at 0.8, 1, 2, 3, 4 and 5% (w/v) and stirred for 12 h to dissolve the polymer completely. The solutions were then placed in an ultrasonic bath for 5 min to remove entrapped air bubbles (Fig. 1). The 0.8% (w/v) concentration was selected for the composites because it gave a viscosity suitable for mixing with the clay dispersions while retaining the film-forming capacity of CMC.

Preparation of clay dispersions and composite aerogels

Laponite, halloysite and kaolin were used as fillers. Aqueous dispersions of each clay were prepared separately at 0.4, 0.8, 1.2, 1.6 and 2.0% (w/v) in 5 mL of deionized water and stirred magnetically at 300 rpm for 12 h. The 0.8% (w/v) CMC solution used for the composites was prepared by magnetic stirring at 60°C until the polymer had dissolved completely.

Each clay dispersion (5 mL) was then mixed with 5 mL of the 0.8% (w/v) CMC solution, giving final concentrations of 0.4% (w/v) CMC and 0.2–1.0% (w/v) clay (CMC:clay mass ratios from 1:0.5 to 1:2.5), and the mixtures were stirred at 300 rpm for 24 h at room temperature. Air bubbles were removed in an ultrasonic bath for 5 min. The composites are designated CMC-H, CMC-K and CMC-L for halloysite, kaolin and Laponite, respectively, followed by 1–5 for clay dispersion concentrations of 0.4, 0.8, 1.2, 1.6 and 2.0% (w/v); the neat aerogel is designated CMC.

Molding and freeze-drying

The solutions were poured into the wells of 12-well plates (well diameter about 22 mm), each well being filled completely, and left to rest for 1 h. The samples were frozen at − 80°C for two nights and then freeze-dried in a freeze dryer (BKFD10S, Biobase Biodustry (Shandong) Co., Ltd., China). Sublimation of the ice under vacuum leaves a porous solid network.

Characterization

Heat-transfer test

Heat transfer through the samples was evaluated with an infrared thermal camera (UTi730E, UNI-T, China; 320 × 240 pixels, thermal sensitivity ≤ 65 mK, measurement range − 40 to 400°C, accuracy ± 2°C or ± 2% of the reading). The emissivity was left at the default setting of the camera (0.95), and the camera was held about 10 cm above the samples.

Before testing, the samples were kept in an oven at 80°C so that all started from the same, uniform temperature. A metal plate was heated to 200°C on a hot-plate magnetic stirrer, and its temperature was confirmed to be stable. The samples were placed on the plate, and their top-surface temperatures were recorded after 0.5, 5, 15 and 30 min. A lower top-surface temperature after a given time indicates slower heat transfer through the sample. Temperatures are reported as mean ± SD of three measurements.

FTIR spectroscopy

Fourier-transform infrared (FTIR) spectra were recorded in attenuated total reflectance (ATR) mode on a PerkinElmer spectrometer (PerkinElmer, Waltham, MA, USA) from 4000 to 450 cm^{-1} at a resolution of 4 cm^{-1} with 6 scans. For each clay, the composites with the lowest and highest clay concentrations (CMC-H1, CMC-H5, CMC-K1, CMC-K5, CMC-L1 and CMC-L5) were analyzed. Small pieces were cut from each sample for analysis.

Compression test

Compressive behavior was measured with a laboratory-built uniaxial compression tester at Istanbul Medeniyet University. Cylindrical samples (14.2–20.7 mm in diameter) were placed on the lower plate and compressed by the upper plate at 1 mm min^{-1} with a 50 kg (490 N) load cell (accuracy ± 0.3% of full scale).

Load and crosshead displacement were recorded continuously; the displacement was obtained from the motor step count (0.00062 mm per step). The diameter of each sample was measured with a digital caliper before testing, and the stress was calculated from the force and the initial cross-sectional area. Contact was taken as the first point from which the stress remained at or above 0.5 kPa. The heights of the freeze-dried samples were not measured before testing. Recording started once the upper plate had touched the sample, and the tester stops automatically when the upper plate is 2.40 mm above the lower plate; the initial height (h_0) of each sample was therefore calculated as the displacement from contact to the end of the test plus 2.40 mm, and the compressive strain as the displacement divided by h_0. Because the tests ended at different strains (40–77%) and the stress rises steeply near densification, the samples were compared at a fixed strain: the stress at 10% strain (σ_{10}) and the compressive modulus, taken as the slope of the stress–strain curve between 2 and 10% strain, are reported. The maximum stress at the end of each test (σ_{max}) depends mainly on how far the sample was compressed and is therefore given only in Table S2 of Online Resource 1. An approximate density of each sample was estimated from the solids in the full volume of one well (7.6 mL), the measured diameter and the calculated height (Table S3 of Online Resource 1); for one CMC-L4 sample whose height, diameter and mass were measured directly, the measured density (29 mg cm^{-3}) was within the range of the estimates for CMC-L4 (34 ± 11 mg cm^{-3}). Three samples were analyzed for each halloysite and kaolin composition, except CMC-K1, for which two valid measurements were available. The Laponite composites were tested in four sessions,

which gave four to seven samples per composition; all valid measurements are reported. The tests were performed at 23 ± 2°C and 62 ± 2% relative humidity.

Statistical analysis

Results are given as mean ± SD. For each clay, the effect of concentration on σ_{10}, the compressive modulus and the calculated height was tested by one-way analysis of variance (ANOVA). Because the variances differed strongly between concentrations, especially for Laponite, Welch's ANOVA, which does not assume equal variances, is also reported, and monotonic trends were tested with Spearman's rank correlation. Pairwise comparisons, including comparisons between clays at the same concentration, were made with Welch's t-test and are reported without correction for multiple comparisons. Top-surface temperatures were compared within each clay series, including neat CMC, by one-way ANOVA followed by Tukey's honestly significant difference (HSD) test. The significance level was 0.05 for all tests.

Use of generative AI

During the preparation of this manuscript, the authors used Claude.ai (Anthropic) solely to check grammar in the written text. No generative AI tool was used for data generation, analysis, or interpretation. The authors reviewed and edited the AI-assisted output and take full responsibility for the content of the publication.

Results and discussion

Shrinkage of the CMC network during freeze-drying

All samples were cast from the same volume (7.6 mL), but their heights after freeze-drying, calculated from the compression tests, differed markedly with clay type (Table S2 of Online Resource 1): 4.0–6.8 mm (5.1 ± 0.8 mm) for halloysite, 4.7–7.7 mm (6.4 ± 1.0 mm) for kaolin and 8.2–10.3 mm (9.7 ± 0.6 mm) for Laponite (Welch's t-test, $p < 0.01$ for all pairs). The CMC–Laponite aerogels therefore retained about 37% of their cast volume, compared with about 20% for the CMC–halloysite and CMC–kaolin aerogels, and their estimated densities were the lowest of the three series (Table S3 of Online Resource 1). Within each series, the height increased slightly with clay concentration (Spearman's $\rho = 0.55–0.64$, $p \leq 0.042$). During freezing, the growing ice crystals concentrate the polymer and the clay into thin walls, and during drying these walls must support themselves; a weak network partly collapses, and the aerogel shrinks (Gawryla et al. 2009). The much smaller shrinkage with Laponite suggests that Laponite reinforced the CMC network already before drying, whereas halloysite and kaolin did not prevent its contraction. Because the heights were calculated from the travel of the upper plate rather than measured, and neat CMC was not included in these tests, the values compare the clays with each other but not with the neat CMC aerogel.

Heat transfer through the aerogels

The top-surface temperatures on the 200°C plate depended on both the type and the concentration of the clay (Fig. 2; the values at 0.5, 5, 15 and 30 min are given in Table S1 of Online Resource 1). After 30 min, the neat CMC aerogel reached 90.1 ± 0.6°C. The differences between samples were largest at the start of heating: after 0.5 min, CMC-K1, CMC-K4, CMC-L4 and CMC-L5 (64.1–65.5°C) were 13.6–15.0°C cooler than neat CMC (79.1 ± 0.5°C). The effect of clay concentration was not monotonic for any of the three clays.

In the Laponite series, the two lowest concentrations (CMC-L1 and CMC-L2) reached 99.0 ± 0.5 and 97.7 ± 0.3°C after 30 min, that is, heat was transferred faster than through neat CMC. CMC-L3 (90.4 ± 0.2°C) and CMC-L4 (89.3 ± 0.2°C) did not differ significantly from neat CMC, whereas CMC-L5 reached 85.3 ± 0.2°C, 4.8°C lower. In the halloysite series, CMC-H1 (89.4 ± 0.2°C) did not differ significantly from neat CMC, CMC-H2 (92.0 ± 0.3°C) and CMC-H4 (92.5 ± 0.4°C) were significantly warmer, CMC-H3 (91.1 ± 0.6°C) did not differ significantly, and CMC-H5 reached the lowest value of the series, 82.9 ± 0.3°C. In the kaolin series, the lowest values were found for CMC-K3 (81.6 ± 0.6°C) and CMC-K4 (82.7 ± 0.4°C), which did not differ significantly from each other, whereas CMC-K5 (89.4 ± 0.7°C) did not differ significantly from neat CMC. CMC-L5, CMC-H5, CMC-K3 and CMC-K4 were all significantly cooler than neat CMC after 30 min (Tukey's HSD test, $p < 0.05$).

Because porosity and pore structure were not measured and density could only be estimated, these differences cannot be assigned with certainty to a single mechanism. In freeze-dried clay–polymer aerogels, the ice crystals template a lamellar structure whose wall thickness and connectivity depend on the solids content and on how the filler interacts with the polymer (Gawryla et al. 2009). Heat is transferred through such materials by conduction through the solid walls and the gas in the pores and by radiation, and finer, more tortuous structures usually reduce it (Wicklein et al. 2015; Fleury et al. 2020). A plausible explanation for the low temperatures of CMC-H5, CMC-K3 and CMC-K4 is that tubular and plate-like particles lengthen the solid conduction path, whereas the higher temperatures at low Laponite loadings may reflect a coarser or more open structure. The CMC–Laponite samples used for compression were also the thickest (see the previous section); if the samples used in this test shrank in the same way, the higher temperatures at low Laponite loadings cannot be explained by thinner samples and are more likely related to the structure of the CMC–Laponite network. The rise for CMC-K5 could arise from clay aggregation at high loading. These explanations need to be confirmed by scanning electron microscopy and porosity measurements. The top-surface temperature also depends on the height of the sample after freeze-drying and on its contact with the hot plate, so these values allow comparison between samples but are not a substitute for thermal conductivity measurements.

Compressive behavior

All samples showed the stress–strain behavior typical of porous materials, with a region of gradual stress increase followed by a steep rise as the structure densified (Fig. 3a–c). The tests ended at strains of 40–65% for halloysite, 49–69% for kaolin and 71–77% for Laponite. Because the stress rises steeply

near densification, the maximum stress at the end of a test mainly reflects how far the sample was compressed, and the samples were therefore compared at 10% strain (Fig. 3d; Table 1).

At 10% strain, the halloysite (1.20–1.55 kPa) and kaolin (1.30–1.42 kPa) composites carried similar stresses (all concentrations pooled, 1.32 ± 0.17 and 1.36 ± 0.11 kPa; $p = 0.38$), and clay concentration had no significant effect for either clay (one-way ANOVA $p = 0.052$ and 0.861; Welch's ANOVA $p = 0.432$ and 0.853). In the Laponite series, σ_{10} increased from 2.57 ± 0.70 kPa at 0.4% to 10.30 ± 7.22 kPa at 2.0% (Welch's ANOVA $p = 0.016$; Spearman's $\rho = 0.56$, $p = 0.002$); the one-way ANOVA, which is less suitable for these unequal variances, gave $p = 0.052$. At every concentration, σ_{10} of the Laponite composites was higher than that of the halloysite and kaolin composites, by factors of 2.0–6.6 and 2.0–7.7, respectively (Welch's t-test, $p = 0.001$–0.031). Across all concentrations, the Laponite composites (6.1 ± 4.9 kPa, $n = 29$) carried about 4.6 times the stress of the halloysite ($n = 15$) and kaolin ($n = 14$) composites ($p < 0.001$). The compressive modulus showed the same pattern (Table S2): 3.2 ± 1.2 kPa for halloysite and 3.1 ± 1.0 kPa for kaolin, without a consistent effect of concentration, whereas for Laponite it increased from 14 ± 8 kPa at 0.4% to 76 ± 52 kPa at 2.0% and was higher than for both other clays at every concentration ($p \leq 0.047$).

The higher stiffness of the Laponite composites is consistent with the ability of Laponite discs to form a physically cross-linked network with polymers through their charged faces and edges (Jin et al. 2018; Tomás et al. 2018). In CMC, the anionic carboxylate groups can bind to the positively charged edges of the discs, so that CMC chains may bridge neighboring discs and form a continuous CMC–Laponite network. Halloysite tubes and kaolinite platelets, whose outer surfaces are mainly negatively charged, interact more weakly with the anionic CMC chains and appear to act mainly as fillers that do not stiffen the CMC network at small deformations (Prasad et al. 1991; Lvov et al. 2008). Because halloysite and kaolinite have nearly the same composition and differ mainly in particle shape, their similar behavior suggests that shape alone had little effect, and that the much stronger effect of Laponite reflects its different chemistry, surface charge, particle size and swelling in water rather than its disc shape. A similar synergy between clay and a polymer or cellulose network in freeze-dried aerogels has been attributed to the formation of a continuous three-dimensional network during ice templating (Gawryla et al. 2009). The same network would explain the smaller shrinkage of the CMC–Laponite aerogels, so their higher stresses did not result from a denser, more collapsed structure. The large scatter of the Laponite composites suggests that their structure was not uniform from sample to sample; the Laponite samples were also prepared and tested in different sessions, which may have contributed to this variation. Because the heights were calculated from the travel of the upper plate rather than measured, the strains and densities are approximate.

Table 1
Compressive stress at 10% strain (σ_{10}, kPa, mean ± SD) of the composite aerogels by clay type and concentration, with one-way and Welch's ANOVA results for each clay

Clay concentration (% w/v)	Halloysite (kPa)	Kaolin (kPa)	Laponite (kPa)
0.4	1.26 ± 0.03 (n = 3)	1.30 ± 0.21 (n = 2)[a]	2.57 ± 0.70 (n = 5)
0.8	1.27 ± 0.10 (n = 3)	1.36 ± 0.19 (n = 3)	3.98 ± 1.23 (n = 7)
1.2	1.20 ± 0.13 (n = 3)	1.38 ± 0.06 (n = 3)	5.95 ± 1.99 (n = 4)
1.6	1.30 ± 0.10 (n = 3)	1.42 ± 0.08 (n = 3)	7.35 ± 5.42 (n = 7)
2.0	1.55 ± 0.21 (n = 3)	1.33 ± 0.09 (n = 3)	10.30 ± 7.22 (n = 6)
One-way ANOVA	F(4, 10) = 3.43, p = 0.052	F(4, 9) = 0.31, p = 0.861	F(4, 24) = 2.75, p = 0.052
Welch's ANOVA	F(4, 4.4) = 1.18, p = 0.432	F(4, 3.7) = 0.32, p = 0.853	F(4, 10.4) = 5.09, p = 0.016

[a] n = 2. The individual values of σ_{10}, the compressive modulus, the calculated height, the strain at the end of each test and σ_{max} are given in Table S2, and the estimated densities in Table S3, of Online Resource 1

FTIR spectroscopy

FTIR spectra of the composites with 0.4 and 2.0% (w/v) clay were used to examine whether the clays were incorporated and how they interact with CMC (Fig. 4).

All composites showed the characteristic bands of CMC: a broad O–H stretching band at about 3330–3370 cm^{-1}, C–H stretching at 2900–2920 cm^{-1}, the asymmetric and symmetric stretching bands of the carboxylate (COO^-) groups at 1592–1595 and 1414–1416 cm^{-1}, and a band at about 1325 cm^{-1} assigned to O–H and C–H bending. At 2.0% clay, the O–H and carboxylate bands of CMC were weaker relative to the clay bands than at 0.4%, as expected from the higher clay content. Because a spectrum of neat CMC was not recorded under the same conditions, shifts of the CMC bands caused by the clays could not be determined. Hydrogen bonding between the hydroxy groups of CMC and the silanol (Si–OH) and aluminol (Al–OH) groups of the clays, and electrostatic or coordination interactions between the carboxylate groups and cations at the clay surfaces, are therefore plausible but were not confirmed, and FTIR alone cannot establish the type or strength of the interactions.

The characteristic clay bands were present in all composites and became stronger from 0.4 to 2.0% clay, showing that the clays were incorporated into the CMC matrix. For halloysite, bands appeared at 3694 and 3622 cm^{-1} (stretching of inner-surface and inner Al–OH groups), at 1027 cm^{-1} in CMC-H1 and 1007 cm^{-1} in CMC-H5 (Si–O stretching), at 910 cm^{-1} (Al–OH bending), at 750 and 686 cm^{-1} (Si–O vibrations) and at 531 and 466 cm^{-1} (Si–O–Al and Si–O–Si deformation) (Joussein et al. 2005; Lvov et al. 2008). For

kaolin, weak Al–OH stretching bands appeared at 3690 and 3620 cm^{-1}, together with bands at 1028 cm^{-1} (Si–O stretching), 913 cm^{-1} (Al–OH bending), 798 cm^{-1} (Si–O vibration) and 534 and 469 cm^{-1} (Si–O–Al and Si–O–Si deformation) (Prasad et al. 1991; Aroke et al. 2013). The kaolin composites also showed a strong, broad band at 1417 cm^{-1} and sharp bands at 877 and 729 cm^{-1}, which are not typical of kaolinite but match the vibrations of carbonate ions, the band at 729 cm^{-1} being characteristic of dolomite. The kaolin used therefore probably contained a carbonate impurity, and the band at 1417 cm^{-1} in these composites cannot be attributed to the carboxylate groups of CMC alone. For Laponite, the Si–O stretching band appeared at 998 cm^{-1} and a band attributed to Mg–O vibrations at 650 cm^{-1} (Xu et al. 2020). Because the Si–O bands of the clays overlap with the C–O stretching bands of CMC (about 1020–1060 cm^{-1}), shifts in this region are difficult to interpret. X-ray diffraction would be needed to confirm that the crystal structures of the clays were retained and to identify the carbonate phase.

Conclusions

The aim of this study was to determine how three clays of different type change the shrinkage, compressive behavior and heat transfer of freeze-dried CMC aerogels, and this aim was achieved for the conditions tested. The CMC–Laponite aerogels retained about 37% of their cast volume, compared with about 20% for the CMC–halloysite and CMC–kaolin aerogels. Compared at 10% strain, the Laponite composites were 2.0–7.7 times stiffer than the halloysite and kaolin composites and became stiffer with increasing Laponite concentration, whereas clay concentration had little effect for halloysite and kaolin. Halloysite and kaolin, which have nearly the same composition but different shapes, behaved similarly, indicating that the chemistry and surface charge of the clay, rather than its shape, determined whether it reinforced the CMC network. Infrared thermography under a fixed thermal load showed that 2.0% halloysite and 1.2–1.6% kaolin lowered the top-surface temperature after 30 min by 7.2–8.5°C relative to neat CMC, whereas low Laponite loadings increased heat transfer, so no single clay gave both the highest stiffness and the lowest heat transfer. FTIR spectra confirmed that the clays were incorporated and indicated a carbonate impurity in the kaolin, but could not establish the type of polymer–clay interaction because neat CMC was not measured under the same conditions.

The work has several limitations. Thermal conductivity, porosity and pore morphology were not measured and density was only estimated, so the thermal results describe relative heat transfer in one test configuration rather than intrinsic insulation performance, and the effect of the clays cannot be separated from that of the higher solids content. Neat CMC was not included in the compression tests, so the shrinkage and stiffness of the composites could be compared only with each other and not with the neat CMC aerogel, and only two to seven samples were tested per composition. The sample heights were not measured but calculated from the travel of the upper plate, from the 2.40 mm gap at which each test stopped, and the fill volume of the wells was not recorded, so the strains and densities are approximate. The Laponite samples were also tested in different sessions and showed large scatter. FTIR spectra were recorded only for the lowest and highest clay concentrations and without a neat CMC reference. Thermal stability, the crystal structure of the clays, biodegradability and the response to

moisture were not studied. Future work should address these points and include cyclic compression tests.

For cellulose research, the results show that, in freeze-dried aerogels of a cellulose ether, the effect of a clay filler depends less on its particle shape than on whether it can form a network with the polymer chains. A swelling, charged clay such as Laponite limited the shrinkage of the CMC network during freeze-drying and stiffened it, whereas the non-swelling 1:1 clays acted mainly as fillers that slowed heat transfer at some loadings. This provides a basis for choosing clays to control the shrinkage and stiffness of CMC and other anionic cellulose-derivative aerogels, for example for packaging or building insulation, once their thermal conductivity and durability have been confirmed.

Statements and Declarations

Author contributions

Onur Aras: Data curation, Investigation, Methodology, Formal analysis.

Samed Ozaydin: Writing – original draft.

Enes Atas: Methodology and Software.

Murat Kazanci: Conceptualization, Methodology, Supervision, Funding acquisition, Resources, Writing – review & editing.

Competing interests

The authors declare that they have no known competing financial interests or personal relationships that could have appeared to influence the work reported in this paper.

Funding: This work was supported by the Council of Higher Education of Türkiye (YÖK) through the 100/2000 doctoral scholarship program and by the Scientific and Technological Research Council of Türkiye (TÜBİTAK) (grant number 112M820).

Data availability

The raw data supporting the findings of this study (thermal imaging records, compression test measurements, and FTIR spectra) have not been deposited in a public repository. These data are available from the corresponding author upon reasonable request.

Acknowledgments: We thank the Science and Advanced Technologies Research Center of Istanbul Medeniyet University (BILTAM) for access to its infrastructure, and Barlanti AlAli and Fatima Ismail for their help with sample preparation and characterization.

References

1. Almasi H, Ghanbarzadeh B, Entezami AA (2010) Physicochemical properties of starch–CMC–nanoclay biodegradable films. Int J Biol Macromol 46:1–5
2. Aras O, Atas E, Kazanci M (2025) Self-reinforced cellulosic nanocomposites: processing optimization and interface characterization of hemp cellulose matrix reinforced with cellulose nanocrystals. Polym Adv Technol 36:e70410
3. Aroke UO, El-Nafaty UA, Osha OA (2013) Properties and characterization of kaolin clay from Alkaleri, North-Eastern Nigeria. Int J Emerg Technol Adv Eng 3:387–392
4. Ataş E, Belet A, Kazanci M (2025) Carboxymethyl cellulose (CMC)-reinforced polyvinyl alcohol (PVA) fibrillar composite membranes: production by centrifugal spinning and characterization. Adv Polym Technol 2025:2382763. https://doi.org/10.1155/adv/2382763
5. Bozoğlan BK, Duman O, Tunç S (2020) Preparation and characterization of thermosensitive chitosan/carboxymethylcellulose/scleroglucan nanocomposite hydrogels. Int J Biol Macromol 162:781–797. https://doi.org/10.1016/j.ijbiomac.2020.06.087
6. Bozoğlan BK, Duman O, Tunç S (2021) Smart antifungal thermosensitive chitosan/carboxymethylcellulose/scleroglucan/montmorillonite nanocomposite hydrogels for onychomycosis treatment. Colloids Surf A 610:125600. https://doi.org/10.1016/j.colsurfa.2020.125600
7. Can V (2008) Synthesis and characterization of polyacrylamide laponite nanocomposite hydrogels. Thesis, Istanbul Technical University
8. Darder M, Aranda P, Ruiz-Hitzky E (2007) Bionanocomposites: a new concept of ecological, bioinspired, and functional composite materials. Adv Mater 19:1309–1319
9. de Oliveira AD, Beatrice CAG (2018) Polymer nanocomposites with different types of nanofiller. In: Nanocomposites—recent evolutions. IntechOpen, London, pp 103–104
10. Fleury B, Abraham E, De La Cruz JA, Chandrasekar VS, Senyuk B, Liu Q, Cherpak V, Park S, ten Hove JB, Smalyukh II (2020) Aerogel from sustainably grown bacterial cellulose pellicles as a thermally insulative film for building envelopes. ACS Appl Mater Interfaces 12:34115–34121. https://doi.org/10.1021/acsami.0c08879
11. Gawryla MD, van den Berg O, Weder C, Schiraldi DA (2009) Clay aerogel/cellulose whisker nanocomposites: a nanoscale wattle and daub. J Mater Chem 19:2118–2124. https://doi.org/10.1039/b823218k
12. Günal B (1999) Increasing the solubility of carboxymethylcellulose. Master's thesis, Istanbul Technical University
13. Jin Y, Shen Y, Yin J, Qian J, Huang Y (2018) Nanoclay-based self-supporting responsive nanocomposite hydrogels for printing applications. ACS Appl Mater Interfaces 10:11033–11042. https://doi.org/10.1021/acsami.8b00806
14. Joussein E, Petit S, Churchman J, Theng B, Righi D, Delvaux B (2005) Halloysite clay minerals—a review. Clay Miner 40:383–426. https://doi.org/10.1180/0009855054040180

15. Keskin B (2016) Production, characterization and application in dye removal of halloysite nanotube-doped ultrafiltration membrane. Master's thesis, Istanbul Technical University
16. López-Angulo D, Bittante AMQB, Luciano CG, Ayala-Valencia G, Flaker CHC, Djabourov M, do Amaral Sobral PJ (2020) Effect of Laponite® on the structure, thermal stability and barrier properties of nanocomposite gelatin films. Food Biosci 35:100596. https://doi.org/10.1016/j.fbio.2020.100596
17. Lvov YM, Shchukin DG, Möhwald H, Price RR (2008) Halloysite clay nanotubes for controlled release of protective agents. ACS Nano 2:814–820. https://doi.org/10.1021/nn800259q
18. Nieto S, Toro N, Robles P, Gálvez E, Gallegos S, Jeldres RI (2022) Flocculation of clay-based tailings: differences of kaolin and sodium montmorillonite in salt medium. Materials 15:1156
19. Özhan HO (2017) Effects of anionic polymer on engineering properties of kaolin clay. Altınbaş University Journal of Engineering Systems and Architecture 1:11–23
20. Prasad MS, Reid KJ, Murray HH (1991) Kaolin: processing, properties and applications. Appl Clay Sci 6:87–119
21. Rahmanian V, Pirzada T, Wang S, Khan SA (2021) Cellulose-based composite aerogels: strategies toward design and functionality. Adv Mater 33:2102892
22. Stenstad P, Andresen M, Tanem BS, Stenius P (2008) Chemical surface modifications of microfibrillated cellulose. Cellulose 15:35–45. https://doi.org/10.1007/s10570-007-9143-y
23. Tomás H, Alves CS, Rodrigues J (2018) Laponite®: a key nanoplatform for biomedical applications? Nanomedicine 14:2407–2420. https://doi.org/10.1016/j.nano.2017.04.016
24. Wan C, Lu Y, Jiao Y, Jin C, Sun Q, Li J (2015) Fabrication of hydrophobic, electrically conductive and flame-resistant carbon aerogels by pyrolysis of regenerated cellulose aerogels. Carbohydr Polym 118:115–118
25. Wicklein B, Kocjan A, Salazar-Alvarez G, Carosio F, Camino G, Antonietti M, Bergström L (2015) Thermally insulating and fire-retardant lightweight anisotropic foams based on nanocellulose and graphene oxide. Nat Nanotechnol 10:277–283. https://doi.org/10.1038/nnano.2014.248
26. Xu P, Erdem T, Eiser E (2020) A simple approach to prepare self-assembled, nacre-inspired clay/polymer nanocomposites. Soft Matter 16:5497–5505. https://doi.org/10.1039/c9sm01585j
27. Yang Y, Chen Y, Leng F, Huang L, Wang Z, Tian W (2017) Recent advances on surface modification of halloysite nanotubes for multifunctional applications. Appl Sci 7:1215. https://doi.org/10.3390/app7121215

Figures

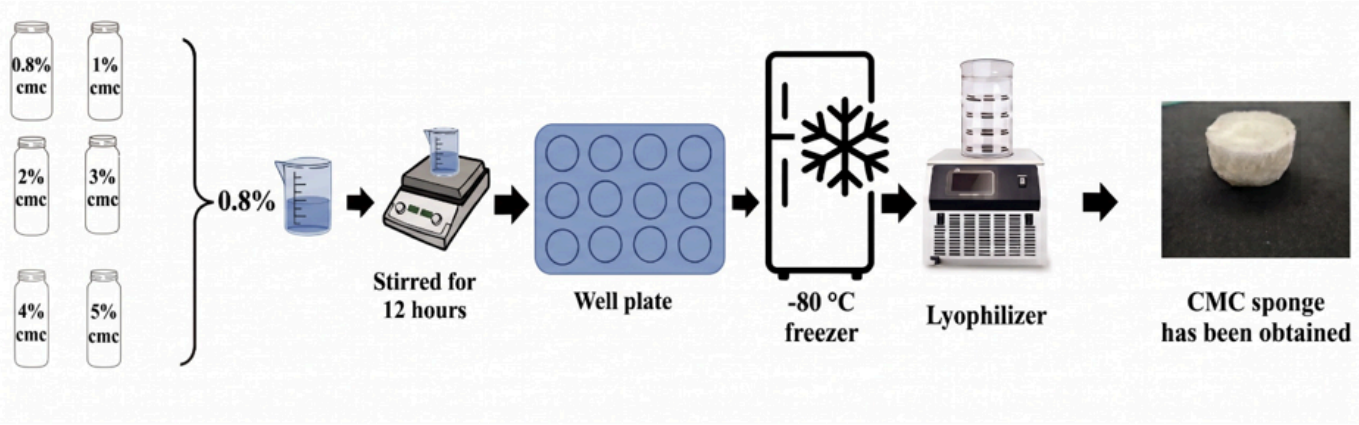


Figure 1

Preparation of the CMC aerogels

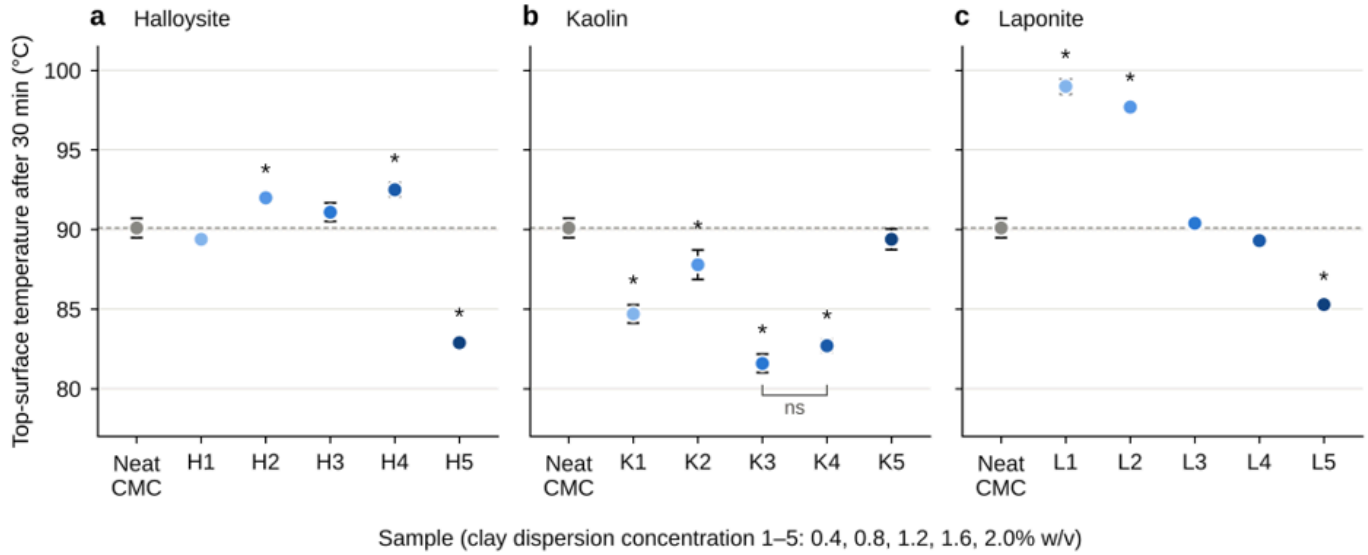


Figure 2

Top-surface temperature after 30 min on a 200 °C hot plate of neat CMC and a halloysite (CMC-H), b kaolin (CMC-K) and c Laponite (CMC-L) composite aerogels (mean ± SD, n = 3). The dashed line marks neat CMC; *, significantly different from neat CMC (one-way ANOVA with Tukey's HSD test, $p < 0.05$); ns, not significant

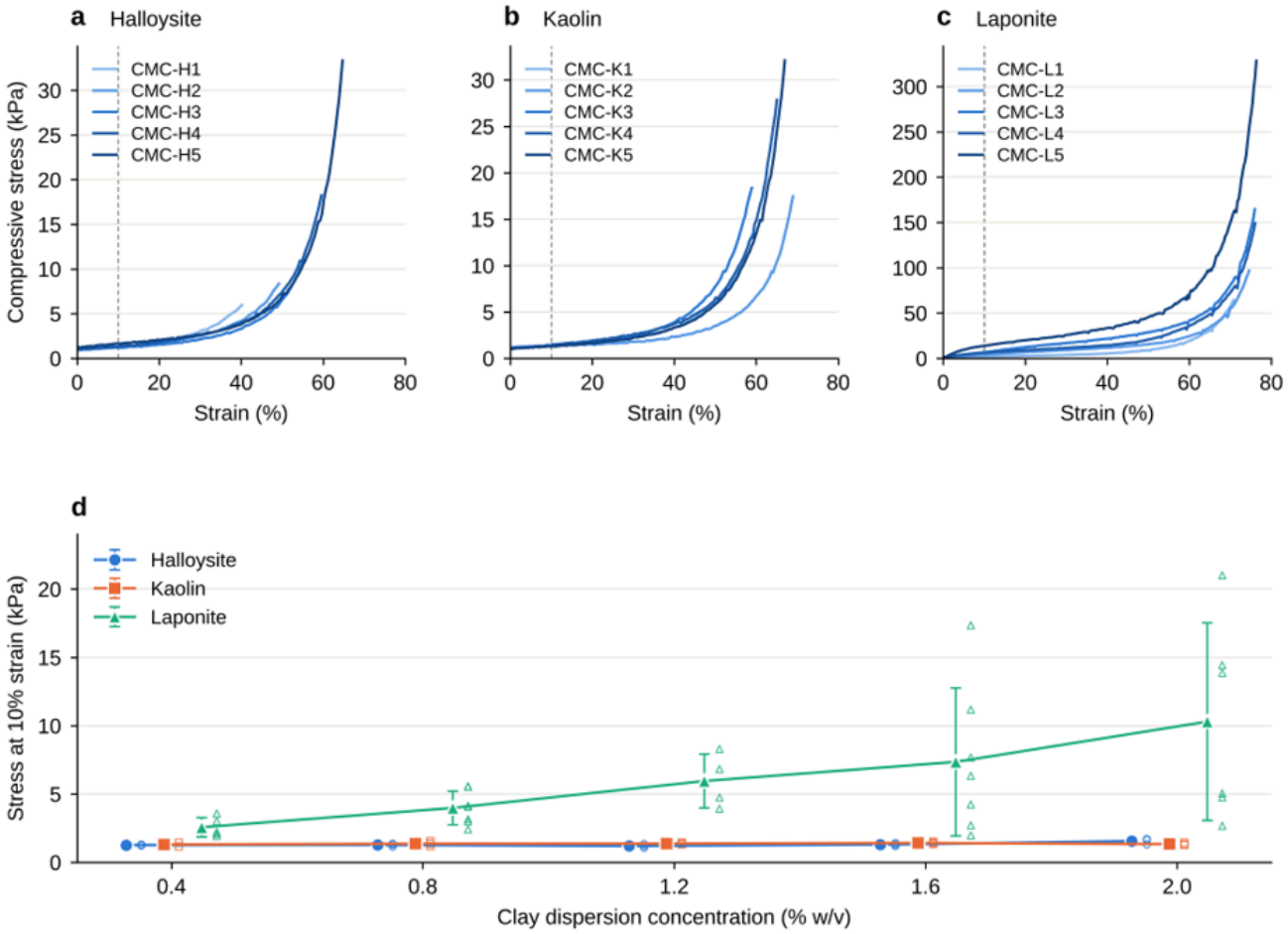


Figure 3

Compressive behavior of the composite aerogels. a–c Representative stress–strain curves of a halloysite (CMC-H1 to CMC-H5), b kaolin (CMC-K1 to CMC-K5) and c Laponite (CMC-L1 to CMC-L5) composites; for each composition the sample with the median σ_{10} is shown, and the dashed line marks 10% strain. Strain was calculated from sample heights estimated from the travel of the upper plate. d Stress at 10% strain (σ_{10}) versus clay concentration (filled symbols, mean ± SD; open symbols, individual samples)

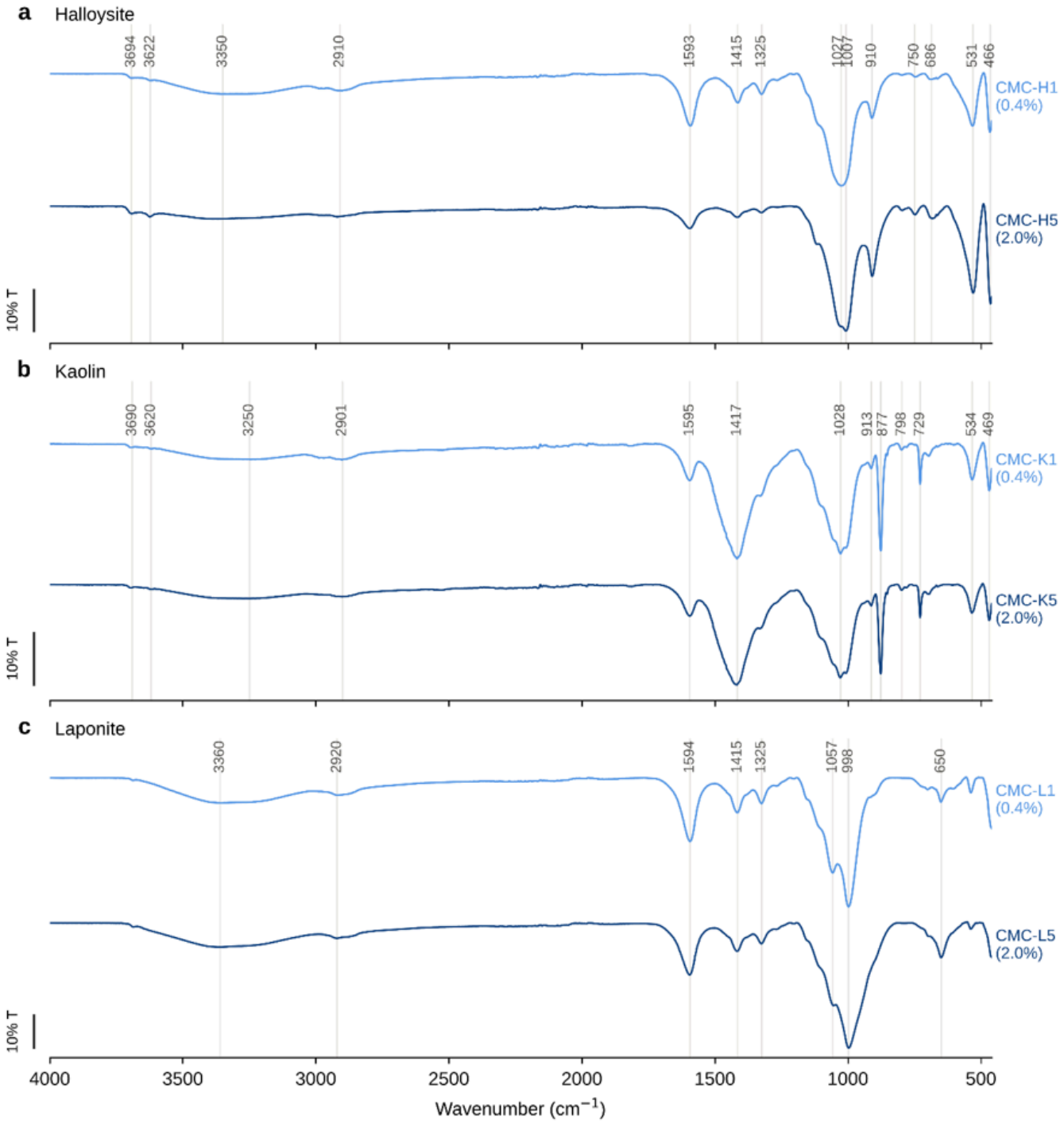


Figure 4

FTIR spectra of the composite aerogels with 0.4 and 2.0% (w/v) clay: a halloysite (CMC-H1, CMC-H5H), b kaolin (CMC-K1, CMC-K5K) and c Laponite (CMC-L1, CMC-L5). Spectra are offset vertically for clarity; vertical lines mark the band positions discussed in the text

Supplementary Files

This is a list of supplementary files associated with this preprint. Click to download.

- OnlineResource..docx